

Dioscorea oppositifolia Mediated Synthesis of Gold and Silver Nanoparticles with Catalytic Activity

Sougata Ghosh^{1*}, Sonal P Gurav¹, Ashwini N Harke¹, Maliyackal Jini Chacko¹, Komal A Joshi², Aarti Dhepe², Chaitanya Charolkar³, Vaishali Shinde³, Rohini Kitture⁴, Vijay Singh Parihar⁵, Kaushik Banerjee⁶, Narayan Kamble⁶, Jayesh Bellare⁷ and Balu A Chopade^{8*}

¹Department of Microbiology, Modern College of Arts, Science and Commerce, Ganeshkhind, Pune-411016, India

²Institute of Bioinformatics and Biotechnology, Savitribai Phule Pune University, Pune-411007, India

³Garware Research Centre, Department of Chemistry, Savitribai Phule Pune University, Pune-411007, India

⁴Department of Applied Physics, Defense Institute of Advanced Technology, Girinagar, Pune-411025, India

⁵New Chemistry Unit, Jawaharlal Nehru Centre for Advanced Scientific Research (JNCASR), Jakkur, Bengaluru 560064, India

⁶National Referral Laboratory, ICAR-National Research Centre for Grapes, Manjri Farm, Pune 412 307, India

⁷Department of Chemical Engineering, Indian Institute of Technology, Bombay, Powai, Mumbai-400076, India

⁸Dr. Babasaheb Ambedkar Marathwada University, Aurangabad-431004, India

Abstract

Biological approaches for synthesis of nanoparticles have gained prime attention in the recent decade as they not only involve lesser time and energy consumption compared to physical and chemical methods but also rapid, efficient and nontoxic. Medicinal plants with diverse phytochemistry have been considered as most promising for development and design of novel routes to synthesize metal nanoparticles. Herein, we report for the first time the synthesis of gold nanoparticles (AuNPs) and silver nanoparticles (AgNPs) using *Dioscorea oppositifolia* tuber extract (DOTE). The synthesis process was complete within 5 h as observed in UV-visible spectroscopy. High resolution transmission electron microscopy revealed that the bioreduced AuNPs were anisotropic exhibiting exotic shaped like nanohexagons, pentagons and blunt ended triangles. Spherical AuNPs ranging from 30 to 60 nm were also spotted. Similarly, distinctly spherical AgNPs without any agglomeration were observed with a size ranging between 17 to 25 nm. Both AuNPs and AgNPs were characterized using various techniques like energy dispersive spectroscopy, X-ray diffraction, dynamic light scattering and fourier transform infrared spectroscopy. Phytochemical analysis employing biochemical tests and GCMS/MS revealed the presence of phenolics, flavonoids, starch, ascorbic acid and citric acid that may help not only in reduction but also in stabilization of the bioreduced nanoparticles. AuNPs and AgNPs synthesized by DOTE exhibited efficient catalytic activity towards reduction of 4-nitrophenol to 4-aminophenol by NaBH4 with a pseudo-first order rate kinetics.

Keywords: *Dioscorea oppositifolia*; Gold nanoparticles; Silver nanoparticles; High resolution transmission electron microscopy; Gas chromatography mass spectrometry; Catalysis

Introduction

Nanostructured materials with tunable properties have gained attention in recent years for development of nanomedicine. Metallic nanoparticles exhibit opto-electronic, chemical and magnetic properties which are of utmost significance towards wide spread applications in catalysis, single electron tunnelling devices, nonlinear optical devices, electron microscopy markers, DNA sequencing and plasmonics [1,2]. Synthesis of gold nanoparticle (AuNPs) and silver nanoparticles (AgNPs) are accomplished traditionally, by physical and chemical methods like UV-irradiation, laser ablation, plasma synthesis, sonochemical and electrochemical reduction. However, these widely used techniques employ harsh chemicals, stringent synthesis conditions, energy and capital intensive and less productive adversities [3]. Moreover, these methods pose environmental threats due to involvement of toxic solvents or additives and lead to overproduction of sludge. Hereby, there is a growing need to design environmentally benign, rapid, efficient, clean, nontoxic and sustainable synthesis procedures. Biological systems have proved to be economical, biocompatible and efficient for synthesis of nanoparticles [4]. Although bacteria, virus and fungi are reported to synthesize metal nanoparticles, medicinal plants have gained much attention and preference owing to their rich phytochemical diversity [5-12]. Hence, we have reported medicinally important plants such as, *Dioscorea bulbifera*, *Gnidia glauca* and *Plumbago zeylanica* for their potential to synthesize various metal nanoparticles [13-19]. However, there are many unexplored medicinal plants in the tribal region which are yet to be studied for

their role in synthesis of exotic metal nanoparticles. One such most significant medicinal plant is *Dioscorea oppositifolia*.

D. oppositifolia is used as a complementary and alternative medicine in the tribal regions of India as well as Zimbabwe. The plant tubers are used as herbal tonic which stimulates the stomach and spleen and exhibits effect on the lungs and kidneys as well. Tubers are eaten to cure poor appetite, chronic diarrhea, asthma, dry coughs, frequent or uncontrollable urination, diabetes and emotional instability. Tubers are also used for topical applications to ulcers, boils and abscesses. Allantoin present in it serves as a cell-proliferant that facilitates healing process. Diosgenin in its roots helps in synthesis of progesterone and other steroid drugs. *D. oppositifolia* is traditionally used as a contraceptive and for treating various disorders of genital organs as well as for arthritis [20,21]. However, there are no thorough scientific

***Corresponding authors:** Sougata Ghosh, Department of Microbiology, Modern College of Arts, Science and Commerce, Ganeshkhind, Pune 411016, India, Tel: 9923268332; E-mail: ghosh.sibb@gmail.com

Balu A Chopade, Dr. Babasaheb Ambedkar Marathwada University, Jaisingpura, Aurangabad 431004, India, E-mail: chopade@unipune.ac.in

Received September 12, 2016; **Accepted** September 16, 2016; **Published** September 23, 2016

Citation: Ghosh S, Gurav SP, Harke AN, Chacko MJ, Joshi KA, et al. (2016) *Dioscorea oppositifolia* Mediated Synthesis of Gold and Silver Nanoparticles with Catalytic Activity. J Nanomed Nanotechnol 7: 398. doi: [10.4172/2157-7439.1000398](https://doi.org/10.4172/2157-7439.1000398)

Copyright: © 2016 Ghosh S, et al. This is an open-access article distributed under the terms of the Creative Commons Attribution License, which permits unrestricted use, distribution, and reproduction in any medium, provided the original author and source are credited.

studies on the optimization and characterization of synthesis processes for nanomaterials with potent therapeutic activity from this plant.

In view of the background, it is of utmost scientific rationale to explore the detailed nanobiotechnological potential of *D. oppositifolia* to synthesize metal nanoparticles like AuNPs and AgNPs with therapeutic applications. Herein, we report for the first time on the synthesis of AgNPs and AuNPs using *D. oppositifolia* tuber extract (DOTE) which were thoroughly characterized. The conditions of the synthetic process were optimized. Further the detailed analysis of DOTE was carried out to understand the mechanism of the synthesis mediated by the key constituents present in the extract. The bioreduced nanoparticles were checked for their efficiency to catalyse chemical reaction.

Materials and Methods

Plant material and preparation of extract

D. oppositifolia tubers were collected from Western Ghats of Maharashtra, India. After chopping the tubers the thin slices were dried in shade for 2-3 days at room temperature. The dried plant material were pulverised into fine powder using an electric blender. *D. oppositifolia* tuber extract (DOTE) was prepared by boiling 5 g of finely ground tuber powder in 100 mL distilled water in a 250 mL Erlenmeyer flask for 5 min. After decantation and centrifugation at 3000 rpm for 10 minutes the extract was filtered through Whatman No.1 filter paper. The filtrate was collected and stored at 4°C for further use [14].

Synthesis and characterization of silver and gold nanoparticles

DOTE mediated synthesis of AuNPs was initiated by addition of 5 mL of DOTE into 95 mL of 1 mM HAuCl₄ solution. The reaction mixture was shaken at 40°C for 5 h in a shaker incubator. Ultraviolet-visible spectrometry operating at a resolution of 1 nm was used at regular intervals to confirm the bioreduction of Au³⁺ ions to AuNPs. Similarly for synthesis of AgNPs 5 mL of DOTE was added into 95 mL of 1 mM AgNO₃ solution. Temperature optimization was carried out in a water bath at 4-50°C with reflux. Concentration optimization was performed by varying the respective salt concentration from 0.3 to 5 mM. The bioreduced nanoparticles were characterized using high resolution transmission electron microscopy (HRTEM), energy dispersive spectroscopy (EDS), X-ray diffraction (XRD) and fourier transform infrared spectroscopy (FTIR) as per our earlier reports [14].

Phytochemicals analysis

Various biochemical assays were employed to determine the

total phenolic, flavonoid, starch, reducing sugar, ascorbic acid and citric acid content of the DOTE as per our earlier report [Ghosh IJN, 2012]. Similarly, GC-MS/MS analysis was used to find out the phytochemical constituents of DOTE [22].

Catalytic activity

The reduction of 4-nitrophenol (4-NP) was carried out using UV-vis spectroscopy at 25°C in a quartz cuvette with an optical path length of 1 cm and volume 4.5 ml. 2 mL of aqueous 4-NP solution (0.1 mM) was mixed with 1.0 mL of freshly prepared NaBH₄ solution (0.1 M) and 0.5 mL of NaOH solution (0.1 M). 25 μL of DOTE synthesized AgNPs (10 mM) were added to the solution. Similar protocol was followed for DOTE synthesized AuNPs as well. The change in absorbance was measured in situ to obtain the successive information about the reaction. Completion of reaction was indicated by the change in color i.e. from yellow to colorless [15,19].

Results

Synthesis and characterization

Synthesis of AuNPs was indicated by the development of ruby red colour on incubation of gold chloride solution with DOTE. The colour changed instantly on adding DOTE which increased upto 5 h indicated by development of intense red colour. UV-visible spectroscopy confirmed the synthesis of AuNPs by showing the peak at 550 nm which increased as a function of time (Figure 1A). Similarly, synthesis of AgNPs was indicated by development of brown colour in the reaction mixture which was initially colourless. UV-visible spectroscopy confirmed the synthesis of AgNPs by indicating the peak at 430 nm which appeared after 1 h of incubation (Figure 1B). The synthesis was completed at 5 h.

Temperature optimization studies confirmed that higher temperature facilitated the rate of synthesis in case of both AuNPs and AgNPs. Rate of synthesis steadily increased from 4°C to 50°C (Figure 2A and 2B). Thus it can be concluded that the rate of bioreduction of metal nanoparticles is temperature dependent.

Concentration optimization studies revealed that 0.5 mM of gold salt solution was optimum for synthesis of AuNPs while higher concentrations showed considerably low rate of synthesis at 550 nm (Figure 3A). However, in case of AgNPs, higher concentrations of AgNO₃ solution facilitated better bioreduction. Maximum synthesis was found for 5 mM followed by 3 mM AgNO₃ concentration (Figure 3B). Concentrations of respective salt solutions were found to play critical role towards the rate of biosynthesis of respective nanoparticles.

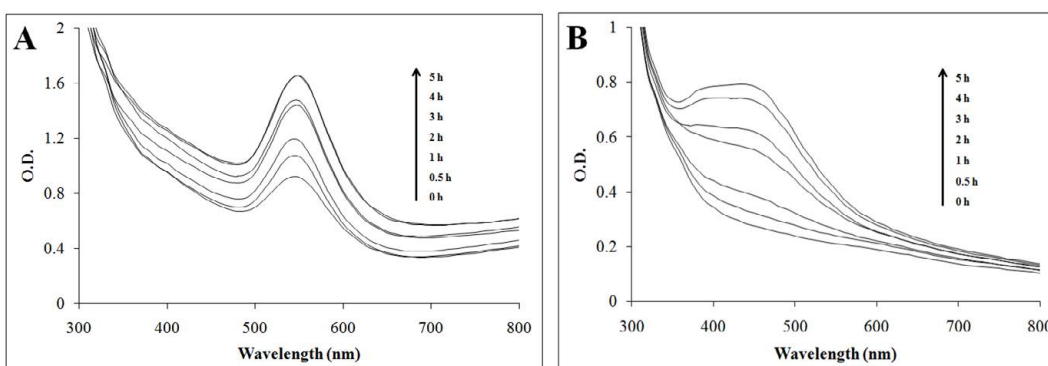


Figure 1: UV-vis spectra recorded as a function of reaction time for nanoparticle formation using DOTE at 40°C with (A) HAuCl₄ solution and (B) 1 mM AgNO₃ solution.

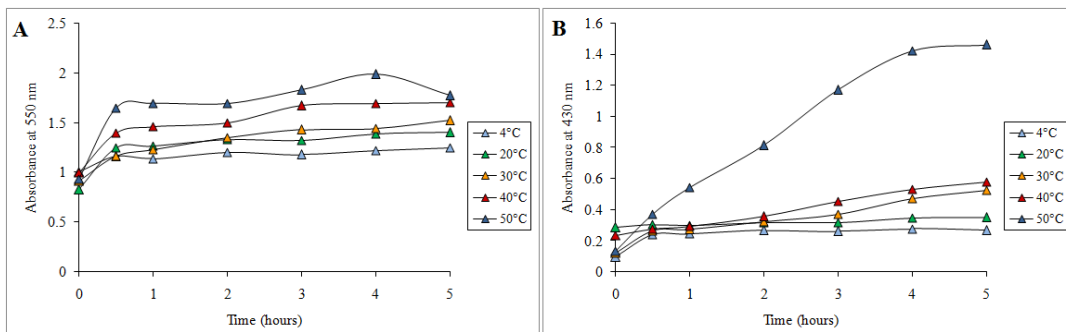


Figure 2: Time course of nanoparticle synthesis using DOTE at different reaction temperatures with (A) 1 mM HAuCl_4 (B) 1 mM AgNO_3 .

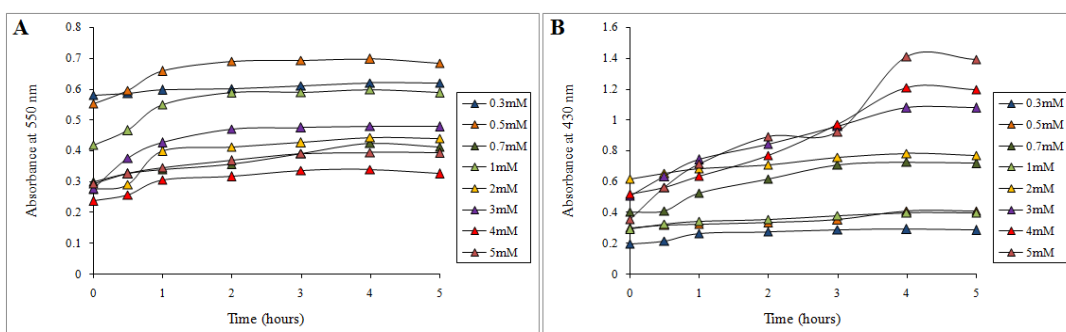


Figure 3: Time course of nanoparticle synthesis using DOTE at 40°C with (A) different concentrations of HAuCl_4 and (B) AgNO_3 .

HRTEM, EDS, DLS analysis

Exotic shapes of AuNPs were observed in HRTEM. The nanoparticles varied in shapes leading to anisotropy. As evident from Figure 4A sharp edged nanohexagons of larger dimensions were observed. Similarly, smaller pentagonal nanoparticles were observed as well beside the hexagons. Blunt ended nanotriangles were also spotted on which nanospheres ranging from 30 to 60 nm along with nanopentagons were closely adhered (Figure 4B). AgNPs were found to be very small distinctly dispersed without any agglomeration (Figure 4C). A thin film of stabilizing material was visible around the AgNPs which might contribute to their stability and dispersion (Figure 4D). AgNPs were found to be spherical in shape ranging between 17 to 25 nm. EDS analysis exhibiting the signature peaks for elemental Au and Ag in the bioreduced nanoparticles confirmed the synthesis of AgNPs and AuNPs, respectively by DOTE (Figure 5A and 5B). Size distribution of bioreduced nanoparticles observed in DLS were also found to be in close agreement with the HRTEM results (Figure 6A and 6B).

The crystalline phase of the AuNPs and AgNPs was confirmed with the XRD. Figure 7A and 7B represent the X-ray diffraction (XRD) data of AuNPs and AgNPs which matches with the JCPDS (Joint Committee for Powder Diffraction Standard) data card no.04-0784 and 04-0783, respectively. Lattice planes (111), (200), (220) and (311) for the NPs show cubic crystalline phase with standard lattice constant to be 4.078 \AA^0 and 4.086 \AA^0 for AuNPs and AgNP, respectively.

FTIR analysis

In order to understand the role of functional groups present of the phytochemicals responsible for reduction of metal ions, FTIR spectra of DOTE was recorded before bioreduction (Figure 8a) and

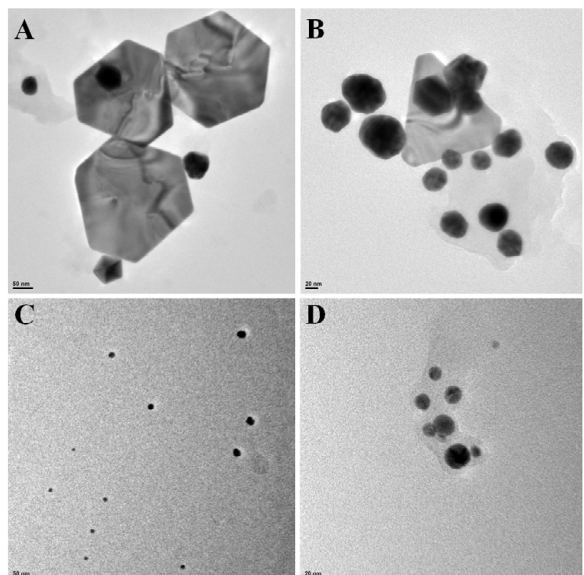


Figure 4: High-resolution transmission electron micrographs of nanoparticles synthesized by DOTE. (A) AuNPs bioreduced by DOTE, inset bar representing 50 nm; (B) Nanospheres and blunt ended gold nanotriangles bioreduced by DOTE, inset bar representing 20 nm; (C) Spherical monodispersed AgNPs synthesized by DOTE, inset bar representing 50 nm; (D) Silver nanospheres synthesized by DOTE, inset bar representing 20 nm.

after reduction of Au^{3+} (Figure 8b) and Ag^{1+} (Figure 8c) into respective NPs. The peaks characteristic to key components like flavonoids and phenolics were observed in Figure 8a. Peaks observed at 1618, 1382,

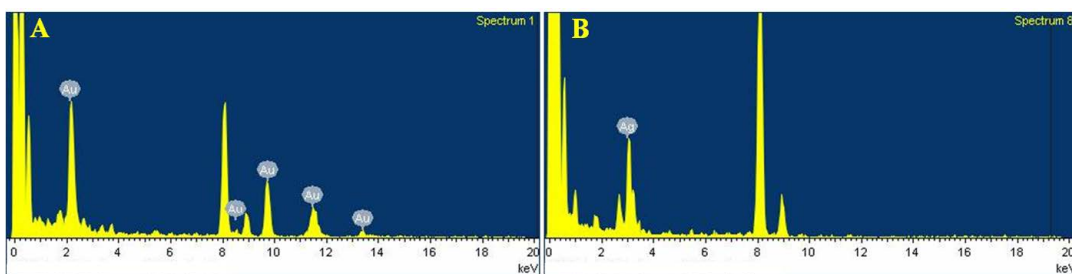


Figure 5: Representative spot EDS profile. (A) AuNPs and (B) AgNPs.

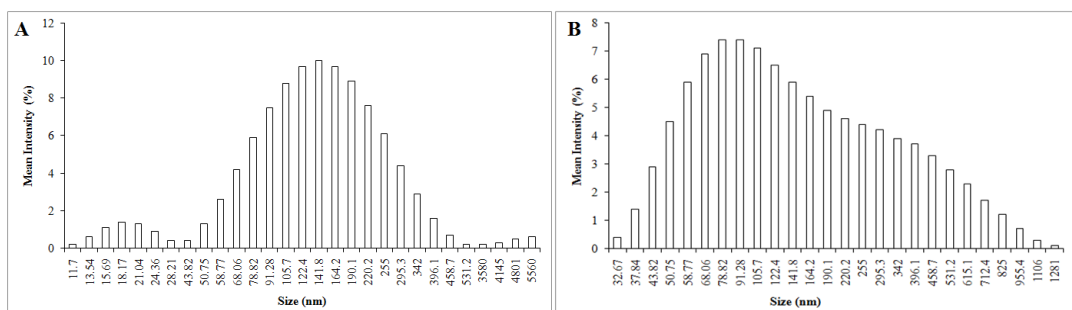


Figure 6: Histogram of size distribution of nanoparticles synthesized by DOTE. (A) AuNPs and (B) AgNPs.

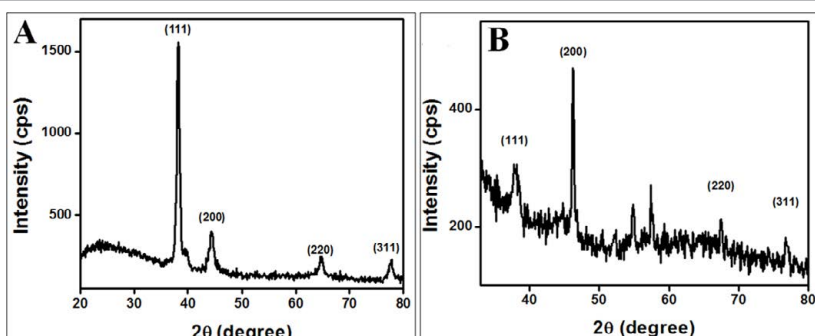


Figure 7: Representative X-ray diffraction profile of thin film (A) AuNPs and (B) AgNPs synthesized by DOTE.

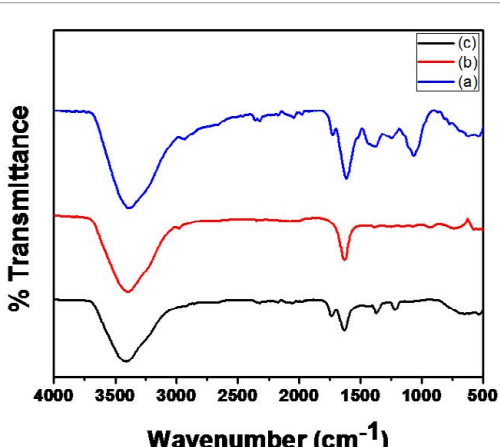


Figure 8: Fourier transform infrared absorption spectra of DOTE before bioreduction (A) and after complete bioreduction of AuNPs (B) and AgNPs (C).

1244 and 1066 cm⁻¹ represent C=N stretch, C-N stretch, C-O stretch. The broad and strong peak at ~3380 cm⁻¹, which is due to hydroxyl (-OH) group of phenols/alcohol, can be seen in the DOTE before and after reduction of both Au³⁺ and Ag¹⁺. Another peak which remained intact after reduction of metal salts represents C=N stretching (~1618 cm⁻¹).

Phytochemical analysis

DOTe exhibited the presence of higher amount of starch followed by phenolic contents. Additionally total reducing sugars ascorbic acid and citric acid were also observed (Table 1). In GCMS/MS analysis diverse groups of phytochemicals were observed major being, Isotridecanol, 2-Isopropyl-5-methyl-1-heptanol and 1-Hexadecanol, 2-methyl (Table 2).

Catalytic activity

The reduction of 4-nitrophenol to 4-aminophenol by NaBH₄ was chosen to study the catalytic performance of both AuNPs and AgNPs

Sample	Total phenolic content ($\mu\text{g/mL}$)	Starch ($\mu\text{g/mL}$)	Total reducing sugars ($\mu\text{g/mL}$)	Ascorbic acid ($\mu\text{g/mL}$)	Citric acid ($\mu\text{g/mL}$)
DOTE	13.33	28.10	3.33	10	1.78

Table 1: Phytochemical composition of DOTE.

Sr. No	Name of compounds	RTS	Formula	Molecular weight
1	Pentanoic acid, 3-methyl-	5.28	$\text{C}_6\text{H}_{12}\text{O}_2$	116
2	Hexanoic acid, 2-methyl-	5.47	$\text{C}_7\text{H}_{14}\text{O}_2$	130
3	Hexanoic acid	6.30	$\text{C}_6\text{H}_{12}\text{O}_2$	116
4	Propionic acid, 3-mercaptop-, isoctyl ester	9.40	$\text{C}_{11}\text{H}_{22}\text{O}_2\text{S}$	218
5	2-Undecanethiol, 2-methyl-	11.84	$\text{C}_{12}\text{H}_{26}\text{S}$	202
6	Phenol, 3-methyl-	12.25	$\text{C}_6\text{H}_8\text{O}$	108
7	3-Buten-2-ol, 4-(2,6,6-trimethyl-2-cyclohexen-1-yl)-	14.37	$\text{C}_{13}\text{H}_{22}\text{O}$	194
8	Z-10-Tetradecen-1-ol acetate	16	$\text{C}_{16}\text{H}_{30}\text{O}_2$	254
9	Octadecane, 6-methyl-	16.27	$\text{C}_{19}\text{H}_{40}$	268
10	Disulfide, di-tert-dodecyl	17.36	$\text{C}_{24}\text{H}_{50}\text{S}_2$	402
11	Tetradecane, 2,6,10-trimethyl-	17.68	$\text{C}_{17}\text{H}_{36}$	240
12	tert-Hexadecanethiol	18.86	$\text{C}_{16}\text{H}_{34}\text{S}$	258
13	1-Hexadecanol, 2-methyl-	19.17	$\text{C}_{17}\text{H}_{36}\text{O}$	256
14	2-Isopropyl-5-methyl-1-heptanol	19.73	$\text{C}_{11}\text{H}_{24}\text{O}$	172
15	Isotridecanol-	20.03	$\text{C}_{13}\text{H}_{28}\text{O}$	200
16	2-Isopropyl-5-methyl-1-heptanol	20.30	$\text{C}_{11}\text{H}_{24}\text{O}$	172
17	Tetradecane	23.03	$\text{C}_{14}\text{H}_{30}$	198
18	10-Heptadecen-8-ynoic acid, methyl ester, (E)-	23.79	$\text{C}_{18}\text{H}_{30}\text{O}_2$	278
19	Phenol, 2,4-bis(1,1-dimethylethyl)-	26.59	$\text{C}_{17}\text{H}_{36}\text{O}$	256
20	3-Chloropropionic acid, heptadecyl ester	31.70	$\text{C}_{20}\text{H}_{39}\text{ClO}_2$	346
21	Oleic Acid	34.37	$\text{C}_{18}\text{H}_{34}\text{O}_2$	282
22	Palmitic acid, (2-phenyl-1,3-dioxolan-4-yl)methyl ester	37.34	$\text{C}_{26}\text{H}_{42}\text{O}_4$	418
23	3-Thiocarbamoyl-1-β-D-ribofuranosylpyrazolo[3,4-d]pyrimidin-4-5H-one	41.01	$\text{C}_{11}\text{H}_{13}\text{N}_5\text{O}_5\text{S}$	327

Table 2: Main compounds detected by GCMS/MS.

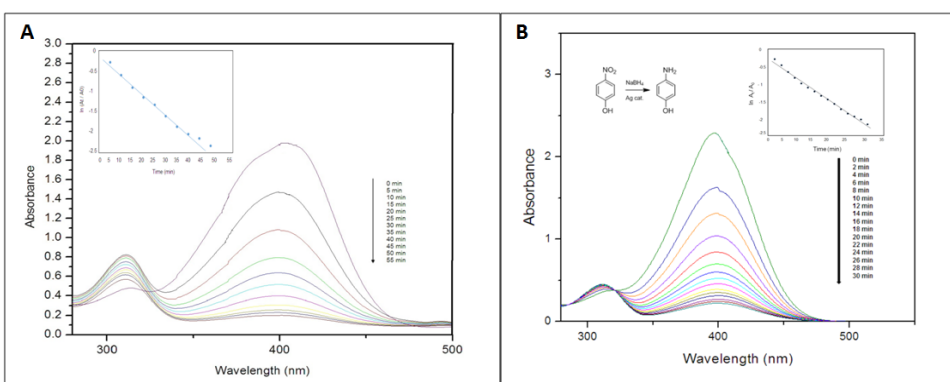


Figure 9: Time dependent UV-vis spectra for monitoring 4-nitrophenol reduction by NaBH_4 catalyzed by A) AuNPs and B) AgNPs synthesized by DOTE. The inset shows the plot indicating the variation of $\ln(\text{At}/\text{A}0)$ vs. time.

(Figure 9A and 9B). When 25 μL of DOTE synthesized AgNPs (10 mM) was used, the reaction was completed in 30 min with the time interval of 2 min. As seen from the Figure 9B, the absorption peak at 400 nm gradually decreased in intensity as the reaction proceeded. At the same time, a new peak of 4 aminophenol at 295 nm appeared and increased in intensity indicated the reduction of 4-NP. Thus, a linear relation between $\ln(\text{At}/\text{A}0)$ versus time t has been obtained as shown in the inset of Figure 9B. The reactions followed pseudo-first order rate kinetics as the concentration of NaBH_4 used exceeded that of 4-NP and AgNPs or AuNPs. This demonstrates a strong catalytic potential of both AuNPs and AgNPs synthesized using DOTE.

Discussion

Medicinal plants are considered to be rich source of bioactive principles which attributes to their promises in development of novel nanomedicine [23-27]. These bioactive principles are reported to have very significant role in the synthesis of nanoparticles and stabilization of the same. Moreover, being medicinal, the plant extracts are non toxic and are proven to be most biocompatible which a prerequisite for design of nanomedicines. *D. oppositifolia* showed complete synthesis of AuNPs and AgNPs within 5 h which is comparable to our previous report on *D. bulbifera* [13,14]. UV-visible spectroscopy confirmed the synthesis showing a peak at 550 nm for AuNPs and 430 nm for AgNPs

which is in agreement with the previous report on synthesis using *Anacardium occidentale* leaf extract [28]. Concentration of the metal salts and the reaction temperature played a major role in the synthesis process which was also reported in case of synthesis of AgNPs using *Cacumen platycladi* extract [29]. HRTEM analysis showed that the exotic shapes of the nanoparticles varied from spherical to truncated triangles which are in well agreement with the report on synthesis of nanoparticles using cape Aloe. It is proposed that such shapes are generated due to slow citric acid reduction [30]. Higher crystalline nature of AuNPs found in XRD also suggested maximum reduction of Au^{3+} into AuNPs, whereas small traces of organic/amorphous phase was seen in XRD of AgNPs which is in well agreement with earlier reports [31-33]. FTIR spectra confirmed the presence of C=N stretch, C-N stretch, C-O stretch and ether linkage that are reported in flavones and catechins [32,34-36]. Presence of a broad and strong peak at $\sim 3380 \text{ cm}^{-1}$, specific to hydroxyl (-OH) group of phenols/alcohol and C=N stretching ($\sim 1618 \text{ cm}^{-1}$) seen in DOTE before and after reduction of both Au^{3+} and Ag^{1+} suggests the role of C=N and -OH in stabilizing the nanoparticles while rest of the groups interacting with the metal salts to reduce them into their respective metal NPs [27]. Phytochemical estimation by biochemical assays and GCMS/MS analysis confirmed the presence of various groups of compounds similar to *D. bulbifera* that might help in the bioreduction like polyphenols, flavonoids, ascorbic acid and citric acid. Similarly the capping agents as starch might add up to its stability [22,37-39]. Both AuNPs and AgNPs synthesized by DOTE showed efficient catalytic activity towards reduction of 4-nitrophenol to 4-aminophenol by NaBH_4 with a pseudo-first order rate kinetics. Our results are in close agreement with earlier reports on *Barleria prionitis*, *Gnidia glauca* and *Breynia rhamnoides* [15,23].

Conclusion

D. oppositifolia, a traditional medicinal plant with curative effect against various ailments is reported herein, to have nanobiotechnological potential. Its tuber extract synthesized both AuNPs and AgNPs within 5 h which is considered to be rapid, efficient and environmentally benign route for synthesis of metal nanoparticles. The bioreduced nanoparticles were characterized and confirmed by various physical techniques and were found to be in a size range between 10 to 30 nm in majority. Various groups of phytochemicals estimated by biochemical methods included polyphenols, starch, reducing sugars, ascorbic acid and citric acid that might help in reduction of the metal ions to nanoparticles and further stabilization as well. The bioreduced AuNPs and AgNPs show chemocatalytic potential in conversion of 4-nitrophenol to 4-aminophenol.

Acknowledgments

The authors acknowledge the help extended for the use of TEM and HRTEM facilities in Chemical Engineering and CRNTS funded by the DST through Nanomission and IRPHA schemes.

References

1. Ghosh S, Patil S, Chopade NB, Luikham S, Kiture R, et al. (2016) *Gnidia glauca* leaf and stem extract mediated synthesis of gold nanocatalysts with free radical scavenging potential. J Nanomed Nanotechnol pp 7: 2.
2. Selvakannan PR, Swami A, Srisathyanarayanan D, Shirude PS, Pasricha R, et al. (2004) Synthesis of aqueous Au core-Ag shell nanoparticles using tyrosine as a pH-dependent reducing agent and assembling phase-transferred silver nanoparticles at the air-water interface. Langmuir 20: 7825-7836.
3. Sant DG, Gujarathi TR, Harne SR, Ghosh S, Kiture R, et al. (2013) *Adiantum philippense* L frond assisted rapid green synthesis of gold and silver nanoparticles. Journal of Nanoparticles pp: 1-9.
4. Singh R, Shedbalkar UU, Wadhwani SA, Chopade BA (2015) Bacteriogenic silver nanoparticles synthesis, mechanism, and applications. Appl Microbiol Biotechnol 99: 4579-4593.
5. Wadhwani SA, Shedbalkar UU, Singh R, Chopade BA (2016) Biogenic selenium nanoparticles current status and future prospects. Appl Microbiol Biotechnol 100: 2555-2566.
6. Singh R, Nawale LU, Arkile M, Shedbalkar UU, Wadhwani SA, et al. (2015) Chemical and biological metal nanoparticles as antimycobacterial agents A comparative study. Int J Antimicrob Agents 46: 183-188.
7. Deshpande P, Gaidhani S, Hitendra M, Shouche Y, Narhe R, et al. (2015) Biosynthesis of gold nanoparticles by human microbiota from healthy skins. J Nanomed Nanotechnol.
8. Gaidhani SV, Yeshvekar RK, Shedbalkar UU, Bellare JH, Chopade BA, et al. (2014) Bio-reduction of hexachloroplatinic acid to platinum nanoparticles employing *Acinetobacter calcoaceticus*. Process Biochem 49: 2313-2319.
9. Wadhwani SA, Shedbalkar UU, Singh R, Karve MS, Chopade BA, et al. (2014) Novel polyhedral gold nanoparticles green synthesis optimization and characterization by environmental isolate of *Acinetobacter* sp SW30. World J Microb Biotechnol 30: 2723-2731.
10. Gaidhani S, Singh R, Singh D, Patel U, Shevade K, et al. (2013) Biofilm disruption activity of silver nanoparticles synthesized by *Acinetobacter calcoaceticus* PUCM 1005. Mater Lett 108: 324-327.
11. Singh R, Wagh P, Wadhwani S (2013) Synthesis, optimization and characterization of silver nanoparticles from *Acinetobacter calcoaceticus* and their enhanced antibacterial activity when combined with antibiotics. Int J Nanomed 8: 4277-4290.
12. Ghosh S, Patil S, Ahire M, Kiture R, Jabgunde A, et al. (2011) Synthesis of gold nanoanisotrops using *Dioscorea bulbifera* tuber extract. J Nanomater 2011: 354793.
13. Ghosh S, Patil S, Ahire M, Kiture R, Kale S, et al. (2012) Synthesis of silver nanoparticles using *Dioscorea bulbifera* tuber extract and evaluation of its synergistic potential in combination with antimicrobial agents. Int J Nanomedicine 7: 483-496.
14. Ghosh S, Patil S, Ahire M, Kiture R, Gurav DD, et al. (2012) *Gnidia glauca* flower extract mediated synthesis of gold nanoparticles and evaluation of its chemocatalytic potential. J Nanobiotechnol 10: 17.
15. Ghosh S, Jagtap S, More P, Shete UJ, Maheshwari NO, et al. (2015) *Dioscorea bulbifera* mediated synthesis of novel $\text{Au}_{\text{core}}\text{Ag}_{\text{shell}}$ nanoparticles with potent antibiofilm and antileishmanial activity. J Nanomater Article ID 562938.
16. Ghosh S, Nitnavare R, Dewle A, Tomar GB, Chippalkatti R, et al. (2015) Novel platinum-palladium bimetallic nanoparticles synthesized by *Dioscorea bulbifera*: anticancer and antioxidant activities. Int J Nanomed 10: 1-4.
17. Ghosh S, More P, Nitnavare R, Jagtap S, Chippalkatti R, et al. (2015) Antidiabetic and antioxidant properties of copper nanoparticles synthesized by medicinal plant *Dioscorea bulbifera*. J Nanomed Nanotechnol 56: 007.
18. Ghosh S, Harke AN, Chacko MJ (2016) *Gloriosa superba* mediated synthesis of silver and gold nanoparticles for anticancer applications. J Nanomed Nanotechnol 7: 4.
19. Padhan B, Panda D (2016) Wild tuber species diversity and its ethno-medicinal use by tribal people of Koraput district of Odisha, India. Journal of Natural Products and Resources 2: 33-36.
20. Poornima GN, Ravishankar RV (2007) In vitro propagation of wild yams *Dioscorea oppositifolia* (Linn) and *Dioscorea pentaphylla* (Linn). African Journal of Biotechnology 6: 2348-2352.
21. Ghosh S, Derle A, Ahire M, More P, Jagtap S, et al. (2013) Phytochemical analysis and free radical scavenging activity of medicinal plants *Gnidia glauca* and *Dioscorea bulbifera*. Plos one 8: e82529.
22. Ghosh S, Chacko MJ, Harke AN, Gurav SP, Joshi KA, et al. (2016) *Barleria prionitis* leaf mediated synthesis of silver and gold nanocatalysts. J Nanomed Nanotechnol 7: 4.
23. Ghosh S, More P, Derle A, Kiture R, Kale T, et al. (2015) Diosgenin functionalized iron oxide nanoparticles as novel nanomaterial against breast cancer. J Nanosci Nanotechnol 15: 9464-9472.
24. Kiture R, Ghosh S, More PA, Date K, Gaware S, et al. (2015) Curcumin-loaded, self-assembled *Aloe vera* template for superior antioxidant activity and trans-membrane drug release. J Nanosci Nanotechnol 15: 4039-4045.

25. Kiture R, Chordiya K, Gaware S, Ghosh S, More PA, et al. (2015) ZnO nanoparticles-red sandalwood conjugate: A promising anti-diabetic agent. *J Nanosci Nanotechnol* 15: 4046-4051.
26. Kiture R, Ghosh S, Kulkarni P, Liu XL, Maity D, et al. (2012) Fe₃O₄-citrate curcumin Promising conjugates for superoxide scavenging tumor suppression and cancer hyperthermia. *J Appl Phys* 111: 064702.
27. Sheny DS, Mathew J, Philip D (2011) Phytosynthesis of Au, Ag and Au-Ag bimetallic nanoparticles using aqueous extract and dried leaf of *Anacardium occidentale*. *Spectrochimica Acta Part A* 79: 254-262.
28. Huang J, Zhan G, Zheng B, Sun D, Lu F, et al. (2011). Biogenic silver nanoparticles by *Cucumis sativus* extract: Synthesis, formation mechanism, and antibacterial activity. *Ind Eng Chem Res* 50: 9095-9106.
29. Krpetic Z, Scari G, Caneva E, Speranza G, Porta F, et al. (2009) Gold nanoparticles prepared using Cape Aloe active components. *Langmuir* 25: 7217-7221.
30. Zhao X, Zhang J, Wang B, Zada A, Humayun M, et al. (2015) Biochemical synthesis of Ag/AgCl nanoparticles for visible-light-driven photocatalytic removal of colored dyes. *Materials (Basel)* 8(5): 2043-2053.
31. Awwad AM, Salem NM, Abdeen AO (2012) Biosynthesis of silver nanoparticles using *Olea europaea* leaves extract and its antibacterial activity. *Nanosci Nanotechnol* 2(6): 164-170.
32. Vivek M, Kumar PS, Steffi S, Sudha S (2011) Biogenic silver nanoparticles by *Gelidiella acerosa* extract and their antifungal effects. *Avicenna J Med Biotechnol* 3: 143-148.
33. Sulochana S, Palaniyandi K, Sivarajanji K (2012) Synthesis of silver nanoparticles using leaf extract of *Andrographis paniculata*. *J Pharmacol Toxicol* 7: 251-258.
34. Gnanajobitha G, Annadurai G, Kannan C (2012) Green synthesis of silver nanoparticle using *Elettaria cardamomum* and assessment of its antimicrobial activity. *Int J Pharma Sci Res* 3(3): 323-330.
35. Preetha D, Arun R, Kumari P, Aarti C (2014) Synthesis and characterization of silver nanoparticles using Cannonball leaves and its cytotoxic activity against MCF-7 cell line. *Journal of Nanotechnology* 6 (8): 164-170.
36. Ghosh S, More P, Derle A, Patil AB, Markad P, et al. (2014) Diosgenin from *Dioscorea bulbifera*: novel hit for treatment of Type II Diabetes Mellitus with inhibitory activity against α-amylase and α-glucosidase. *PLoS One* 9: e106039.
37. Dasgupta S, Banerjee K, Patil SH, Ghaste MS, Dhimal KN, et al. (2010) Optimization and comparison of one- and two dimensional gas chromatography time-of-flight mass spectrometry for separation and estimation of the residues of 160 pesticides and 25 persistent organic pollutants in grape and wine. *J Chromatogr A* 1217: 3881-3889.
38. Banerjee K, Utture S, Dasgupta S, Pradhan S, Kandaswamy C, et al. (2012) Multiresidue determination of 375 organic contaminants including pesticides, polychlorinated biphenyls and polyaromatic hydrocarbons in fruits and vegetables by gas chromatography-triple quadrupole mass spectrometry with introduction of semi-quantification approach. *J Chromatogr A* 1270: 283-295.
39. Gangula A, Podila R, Ramakrishna M, Karanam L, Janardhana C, et al. (2011) Catalytic reduction of 4-nitrophenol using biogenic gold and silver nanoparticles derived from *Breynia rhamnoides*. *Langmuir* 27: 15268-15274.